A Journal of the Gesellschaft Deutscher Chemiker

Angewandte International Edition GDCh Chemie

www.angewandte.org

Accepted Article

Title: Membrane-Anchoring Photosensitizer with Aggregation-Induced Emission Characteristics for Combating Multidrug-Resistant Bacteria

Authors: Huan Chen, Shengliang Li, Min Wu, Kenry Kenry, Zhongming Huang, Chun-Sing Lee, and Bin Liu

To be cited as: *Angew. Chem. Int. Ed.* 10.1002/anie.201907343
Angew. Chem. 10.1002/ange.201907343

Link to VoR: http://dx.doi.org/10.1002/anie.201907343
http://dx.doi.org/10.1002/ange.201907343

WILEY-VCH

10.1002/anie.201907343

WILEY-VCH

COMMUNICATION

Membrane-Anchoring Photosensitizer with Aggregation-Induced Emission Characteristics for Combating Multidrug-Resistant Bacteria

Huan Chen[a], Shengliang Li[b]*, Min Wu[a], Kenry[a], Zhongming Huang[b], Chun-Sing Lee[b]*, and Bin Liu[a]*

Abstract: Traditional photosensitizers (PSs) show reduced singlet oxygen ($^1O_2$) production and quenched fluorescence upon aggregation in aqueous media, which greatly affect their efficiency in photodynamic therapy (PDT). Meanwhile, non-targeting PSs generally yield low efficiency in antibacterial performance due to their short lifetimes and small effective working radii. Herein, a water-dispersible membrane anchor (**TBD-anchor**) PS with aggregation-induced emission is designed and synthesized to provide superefficient $^1O_2$ generation specifically on bacteria membrane. **TBD-anchor** possesses energy donor and acceptor subunits to modulate the bandgap of the PS, and cationic groups were introduced to target bacterial membrane through electrostatic and hydrophobic interactions. **TBD-anchor** showed superefficient antibacterial performance towards both Gram-negative bacteria (*E. coli*) and Gram-positive bacteria (*S. aureus*). Over 99.8% killing efficiency was obtained for Methicillin-Resistant *Staphylococcus aureus* (*MRSA*) when they were exposed to 0.8 μM of **TBD-anchor** at a low white light dose (25 mW/cm^2) for 10 minutes. **TBD-anchor** thus shows great promise as an effective antimicrobial agent to combat the menace of multidrug-resistant bacteria.

Bacterial resistance to conventional antibiotics is one of the most serious healthcare problems faced by the world today.[1] Over the past decades, millions of patients have been affected by various health- and life-threatening bacteria-caused diseases and the situation has deteriorated with the emergence of multidrug-resistant (MDR) bacteria.[2] Unfortunately, the number of infections caused by MDR bacteria has been on the rise.[1b] As noted in the recent World Economic Forum reports, antibiotic-resistance poses a serious threat to global health.[3] Therefore, there is an urgent need for the development of new strategies to resolve this serious healthcare problem.

Traditional methods such as antibiotic treatment and radiotherapy have shown limitations in clinical applications, among which the drug resistance and side effects are the two main obstacles.[2c, 2e] Among the emerging antibacterial therapeutic methods, photodynamic therapy (PDT) has attracted increasing attention.[4] It utilizes photosensitizers (PSs) to produce toxic reactive oxygen species for antibacterial treatment, which has shown great potentials due to the non-invasive nature of PDT, negligible drug resistance, low systemic toxicity and minimal side effects.[2c, 4b, 4c] Conventional PSs, such as TMPyP and Toluidine blue O have been used to kill bacteria with moderate effectiveness.[5] This is because the aggregation of traditional hydrophobic PSs often causes fluorescence quenching with reduced singlet oxygen ($^1O_2$) generation in aqueous media, which significantly hampers their bacteria ablation efficacy.[2a] To address this issue, PSs with aggregation-induced emission (AIE PS) have been developed to show bright fluorescence and excellent $^1O_2$ production in the aggregate state, or even as nanoparticles dispersed in aqueous media.[4d, 4e]

So far, AIE PSs have been successfully used to develop theranostic probes for cancer.[4j, 4k] Detailed studies reveal that their killing efficiency can be significantly enhanced when the probes can selectively target cell organelles, such as cytoplasmic membrane and mitochondria,[6] as compared to those distributed in the cell cytoplasm. This is due to the short lifetimes and small effective radii of the reactive oxygen species.[2c, 7] Motivated by the initial success, we and others have further developed AIE probes to detect and kill bacteria.[4i, 4k, 8] These probes generally share the good feature of light-up response to bacteria, so that the detection can be done in real time without washing steps.[8a] Some of these probes also showed obvious dark toxicity, which combined with light-induced photosensitization to effectively kill bacteria even under sunlight.[8b] Most of these studies did not address specificity among different bacteria. Therefore, bacteria specific theranostic probes have been realized through bioconjugation between AIE PSs and peptides that are specific to certain bacteria. One such example is the AIE-Van probe, which is specific to Gram-positive bacteria.[4i]

The PS sensitivity or its effectiveness in ROS production is highly dependent on its capability in light absorption and intersystem crossing (ISC).[4f] ISC can be adjusted through HOMO-LUMO engineering to realize a small energy gap between the triplet (T1) and singlet (S1) states. However, as AIE PSs generally have rotor structures, poor conjugation is often observed within the molecules, yielding narrow absorption in the short wavelength region.[4h] In this regard, how to design new PSs with broad absorption and large molar absorptivity is in high demand to develop highly effective probes for bacteria detection and ablation.

In this study, we propose an AIE-based membrane-anchoring photosensitizer (**TBD-anchor,** as shown in **Scheme 1**), which was designed to combine two features, i.e., $^1O_2$ generation and bacterial membrane anchoring abilities. The molecular design was started from AP3, since the molecule with D (donor)-A′ (auxiliary acceptor)-π (π spacer)-A (acceptor) structure could offer broad absorption in the visible range with effective $^1O_2$ generation.[4b, 4c] Motivated by the fact that cationic groups could insert effectively into some bacterial membrane,[9] a phenyl ring with three cationic groups was introduced to AP3, which yielded **TBD-anchor** for bacteria imaging and ablation. Detailed studies

[a] Huan Chen, Dr. Min Wu, Dr. Kenry, Prof. Bin Liu
Department of Chemical and Biomolecular Engineering, National University of Singapore, 4 Engineering Drive 4, 117585, Singapore
E-mail: cheliub@nus.edu.sg

[b] Dr. Shengliang Li, Zhongming Huang, Prof. Chun-Sing Lee
Center of Super-Diamond and Advanced Films (COSDAF) Department of Chemistry, City University of Hong Kong, 83 Tat Chee Avenue, Kowloon, Hong Kong SAR, P. R. China.
E-mail: lishengliang@iccas.ac.cn; apcslee@cityu.edu.hk

Supporting information for this article is given via a link at the end of the document.

10.1002/anie.201907343

reveal that **TBD-anchor** has strong $^1O_2$ generation capability with high efficiency in ablating various bacteria.

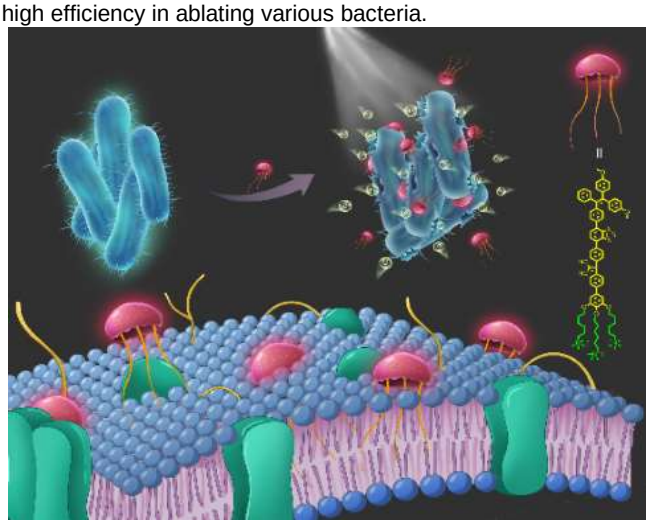

Scheme 1. Chemical structure and schematic illustration of the mechanisms for **TBD-anchor** for bacteria membrane penetration.

The synthetic route to **TBD-anchor** is shown in **Figure S1.** The structures of intermediates and **TBD-anchor** were well characterized with NMR and mass spectrometer (**Figure S2-S9**). **TBD-anchor** shows a very broad absorption from 300 to 500 nm with an emission maximum at 650 nm (**Figure 1a**). As illustrated in **Figure 1b-1c**, the anchor shows nearly no emission in pure methanol solution. With the increase in toluene (a poor solvent of **TBD-anchor**) volume content in the methanol/toluene mixtures from 0 to 60%, slight enhancements in emission intensity were observed. When the toluene fraction was more than 60%, significant emission enhancements centered at 650 nm were noted owing to the aggregate formation of **TBD-anchor** (**Figure 1b**). The result indicates that **TBD-anchor** processes aggregation-induced emission characteristic.

The $^1O_2$ generation capability of **TBD-anchor** was investigated by measuring changes in UV-visible spectra of 9,10-anthracenediyl-bis(methylene)dimalonic acid (ABDA, a $^1O_2$ indicator) upon white light irradiation (400-700 nm, **Figure S10**). Meanwhile, Rose Bengal (RB), a commercial PS, was employed as a reference. As shown in **Figure 1d-f**, the absorbance of ABDA treated with **TBD-anchor** and RB at 378 nm shows obviously attenuation with the irradiation time. Importantly, the absorbance of ABDA in **TBD-anchor** solution is decreased by 74.7% under white light irradiation for 5 min, indicating that 7.47 μmol of ABDA was consumed every min when 5 μM of **TBD-anchor** was exposed to the light. As comparison, only 2.92 μmol of ABDA was consumed for 5 μM of RB under the same condition. Furthermore, the $^1O_2$ generation quantum yield of **TBD-anchor** was calculated to be 0.48 by measuring $^1O_2$ phosphorescence at 1270 nm using RB as a reference (**Figure S11**). It is worth noting that **TBD-anchor** shows excellent photostability in comparison with other typical organic dyes (i.e., RB, Ce6 and ICG) when exposed to white light irradiation because the AIE probe is not easily oxidized by the photogenerated $^1O_2$ (**Figure 1d-1e** and **Figure S12**).

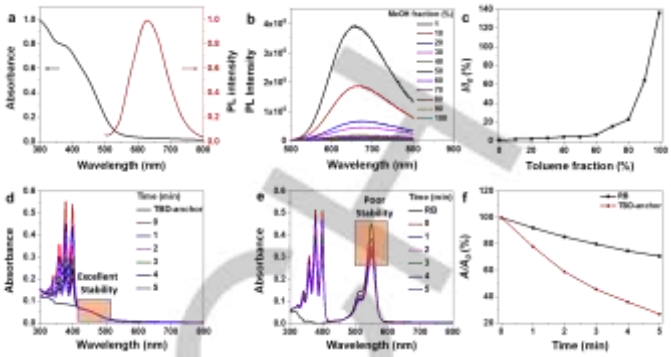

Figure 1. a) UV–vis absorption and photoluminescence (PL) spectra of **TBD-anchor**. b) PL spectra of **TBD-anchor** in MeOH/Toluene mixtures with different toluene fractions (λ_{ex} = 450 nm). c) The plot of relative emission intensity (I/I_0) at 650 nm versus the composition of the MeOH/Toluene mixtures of **TBD-anchor**. UV–vis absorption spectra of ABDA in the presence of **TBD-anchor** (d) and RB (e) under white light irradiation (λ = 400-700 nm). f) Decomposition rates of ABDA in the presence of **TBD-anchor** and RB under light irradiation, where A_0 and A are the absorbances of ABDA at 378 nm. [**TBD-anchor** and RB] = 5 × 10^{-6} M, [ABDA] = 5 × 10^{-5} M. Power of irradiation: 10 mW/cm**²**.

To understand the interaction between **TBD-anchor** and bacteria, *E. coli* cells were used for the imaging experiment by confocal laser scanning microscopy (CLSM) and DAPI (4',6-diamidino-2-phenylindole) was used to stain the bacteria DNA. As shown in **Figure 2a-b** and **Figure S13**, DAPI could stain the bacteria interior with false green color, while the red emission from the exteria of bacterial was due to the staining with **TBD-anchor**. The overlay image (**Figure 2c**) clearly shows that the outer bacterial layer is red and the interior is green, suggesting that **TBD-anchor** could effectively anchor to the bacterial membrane. The zeta potential of *E. coli* was negative (-13.3 mV), which was increased to positive (15.6 mV) when 5 μM of **TBD-anchor** was added to the *E. coli* mixture (**Figure S14**). This result suggests that **TBD-anchor** could effectively bind to bacteria.[9a, 10]

A standard Isothermal Titration Calorimetry (ITC) assay was then performed to further investigate the binding mechanism of **TBD-anchor** to bacterial membrane. The observed enthalpy (ΔH_{obs}) varied distinctively with the addition of the anchor (**Figure S15**), indicating its effective interaction with *E. coli* [11]. The negative ΔH_b (-48.6) and ΔS_b (-35.5) suggest electrostatic interactions between **TBD-anchor** and bacteria.[11b, 12] The binding enthalpy varied from negative to around zero after the anchor addition, indicating hydrophobic interactions.[12b] Therefore, **TBD-anchor** could effectively interact with *E. coli* through both electrostatic and hydrophobic interactions.

10.1002/anie.201907343

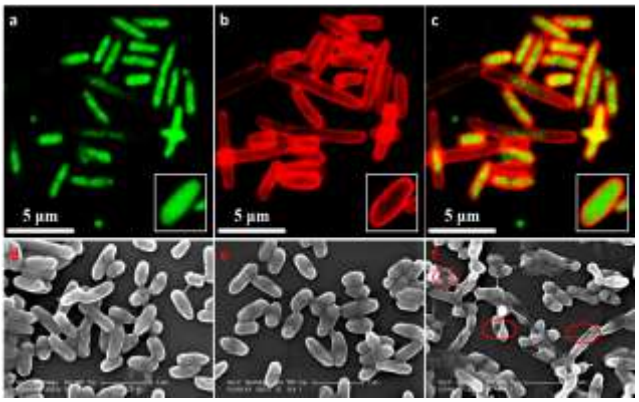

Figure 2. Interaction between **TBD-anchor** and *E. coli*. CLSM images of *E. coli* cells treated with 10 μM **TBD-anchor** in PBS. a) The bacterial inner parts were labeled by DAPI with false green color. b) Red emission of the bacterial membranes stained with **TBD-anchor**. c) Overlay images of a and b. SEM Images of *E. Coli* affiniting with **TBD-anchor**. d) Blank *E. Coli*, e) *E. Coli* treated with 10 μM **TBD-anchor** under dark condition, f) *E. Coli* treated with 10 μM **TBD-anchor** under whitle light.

The morphologies of bacteria with or without **TBD-anchor** treatment were obtained by scanning electron microscopy (**Figure 2d-f**). The control *E. coli* (without **TBD-anchor** treatment or treated with **TBD-anchor** in the dark) showed smooth outer surfaces. However, the outer surfaces of *E. coli* treated with **TBD-anchor** after irradiation were significantly destroyed, thereby illustrating the bio-impact of the localized generation of $^1O_2$ rooted from **TBD-anchor**.[9a]

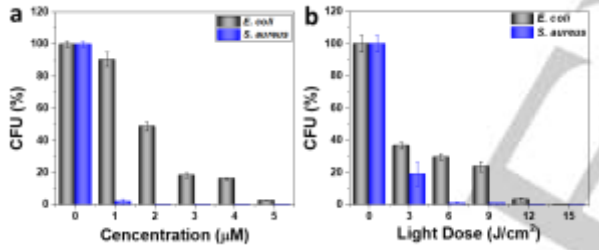

Figure 3. Antibacterial activity of **TBD-anchor** towards *E. coli* and *S. aureus*. a) CFU (colony forming unit) inhibition of *E. coli* and *S. aureus* with a dose of 15 J/cm^2. b) Inhibition of **TBD-anchor** towards *E. coli* and *S. aureus* under different light doses irradiation.

As **TBD-anchor** possessed highly effective $^1O_2$ generation ability, it motivated us to investigate their antibacterial PDT ability. The antibacterial activities of **TBD-anchor** towards Gram-negative *E. coli* and Gram-positive *S. aureus* were examined by irradiation under white light (400-700 nm). The standard plate colony counting method was used to determine the percentage of live bacteria. The results show that the percentage of live bacteria decreases significantly with the increasing of **TBD-anchor** concentrations upon 15 J/cm^2 (irradiation for 10 min at a fluence of 25 mW/cm^2) of white light irradiation. Approximately 96% of *E. coli* is inhibited when treated with 5 μM of the **TBD-anchor** and 2 μM of the anchor can destroy 99.5% of *S. aureus* (**Figure 3a** and **Figure S16-S17**). The results indicate that **TBD-anchor** holds excellent antibacterial activity towards both Gram-positive and Gram-negative bacteria at low PS concentration upon very low-dose irradiation, suggesting that **TBD-anchor** is a broad spectrum antibacterial probe. Under the dark condition, negligible toxicity was observed when 40 μM **TBD-anchor** was used to treat *E. coli* and *S. aureus* (**Figure S18**). It is also noted that even 32 μM **TBD-anchor** has negligible toxicity towards healthy NIH 3T3 cells under both dark and light conditions, which strongly indicates that **TBD-anchor** is biocompatible (**Figure S19**).

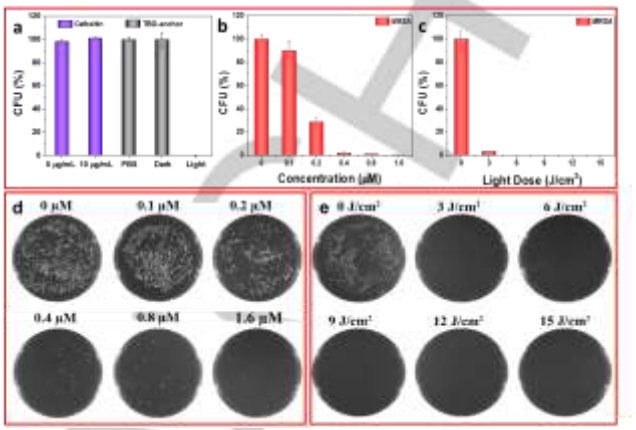

Figure 4. Antibacterial activity of **TBD-anchor** towards *MRSA*. a) Inhibition of *MRSA* growth by **TBD-anchor** at 10 μM and Cefoxitin with or without light with a dose of 15 J/cm^2. b) Inhibition of bacteria growth under light irradiation with a dose of 15 J/cm^2 at different PS concentrations. c) Antibacterial activity of **TBD-anchor** towards *MRSA* under different light doses irradiation. d) Images of CFU for *MRSA* on agar plate after 5 min treatment with different concentrations of the **TBD-anchor** and e) treatment with 1 μM **TBD-anchor** under different light doses irradiation.

It is well known that *MRSA* is one of the most dangerous drug-resistant bacteria which could induce clinical death immediately.[1b] We next sought to systematically determine the antibacterial activity of **TBD-anchor**. As shown in **Figure 4a** and **Figure S20**, > 99.9% of *MRSA* were killed upon treatment with 10 μM of **TBD-anchor** under a light dose of 15 J/cm^2. As a control, no significant inhibition was found in the PBS- and Cefoxitin (a second-generation antibiotic used to treat a wide variety of bacterial infections)-treated groups, even when the Cefoxitin concentration was increased to 10 μg/mL (≈ 23.3 μM). The excellent antibacterial activity of **TBD-anchor** in inhibiting the growth of *S. aureus* and *MRSA* cells motivated us to further investigate the antibacterial activity at low concentrations. **Figures 4b** and **4d** illustrate that > 98.1% of *MRSA* were killed at 0.4 μM and the inhibition ability was increased to 99.8% at 0.8 μM with 15 J/cm^2 irradiation, respectively. For the killing ability of *S. aureus* (**Figure S21-S22**), the inhibition percentage is up to > 96.4% at 0.4 μM and 99.3% at 0.8 μM, respectively. This compares favorably to other commercial PSs. For example, the concentration of Toluidine blue O used for inhibiting ≥ 99.0% of *MRSA* and *S. aureus* is up to 80 μM under a dose of 30 J/cm^2.[5b] For Ce6, the concentration is up to 40 μM to kill 99.9% of *S. aureus* and *MRSA* with a dose of 15 J/cm^2.[4l] The comparison strongly suggests that **TBD-anchor** is an excellent antibacterial PDT agent.

Thanks to the excellent antibacterial activity, the antibacterial PDT performance of **TBD-anchor** at 5 μM, 2 μM and 1 μM against the growth of *E. coli*, *S. aureus,* and *MRSA* was further examined by varying the irradiation dose, respectively. As shown in **Figure 3b**, **Figure 4c**, **Figure 4e** and **Figure S23-S24**, > 99.9% of all three bacteria were destroyed at a dose of 15 J/cm^2. The inhibition ability toward *S. aureus* was 91.1% at an irradiation of 3 J/cm^2 and the value was increased to > 99.1% when the dose was 6

J/cm^2. More importantly, 96.8% of *MRSA* were killed with an irradiation dose of 3 J/cm^2 and the killing ability was increased to 100% at a dose of 6 J/cm^2. It is worth noting that the light dose needed to kill *E. coli*, *S. aureus* and *MRSA* cells with **TBD-anchor** was significantly lower than those based on porphyrin, as described in the literature (30–266 J/cm^2)[13] and XF-73 (13.7–15.2 J/cm^2) which is in phase 1 clinical trial as treatment for nasal decolonization of *S. aureus* (including *MRSA*).[14] To the best of our knowledge, this is the first AIE PS which can effectively ablate bacteria below micro-molar concentration.[4g, 4j] The antibacterial performance of **TBD-anchor** is superior to many reports in the literature, such as conjugated polyelectrolyte based system[9a] and other non-AIE PSs.[15] Therefore, **TBD-anchor** is one of the most effective antibacterial photosensitizers reported so far (**Table S1**).[2c, 4g]

In summary, we developed an AIE PS (**TBD-anchor**) with very efficient $^1O_2$ generation for membrane-targeted antibacterial treatment, which has achieved multidrug-resistant bacteria suppression at the nano-molar level. Due to its AIE backbone with electron-donor and electron-acceptor structural units, **TBD-anchor** shows broad absorption in the visible range, while three cationic groups were introduced into the molecular design for bacterial membrane anchoring. Fluorescence imaging and ITC results confirm that **TBD-anchor** interacts with bacterial cell membranes through both electrostatic and hydrophobic interactions. **TBD-anchor** also shows effective $^1O_2$ generation with a $^1O_2$ quantum yield of 0.48. Benefitting from the enhanced membrane interactions and photosensitizing ability, **TBD-anchor** exhibited super-efficient antibacterial capability in destroying *S. aureus* and *MRSA* at low concentration (1-2 μM) and low light dose (3-6 J/cm^2). Interestingly, the anchor also exhibited a strong capability in killing *S. aureus* and *MRSA* at 0.4 μM under white light of 15 J/cm^2. Our study has demonstrated the promising potential of AIE PS and the anchor strategy for anti-*MRSA* treatment.

Acknowledgements

We thank the Singapore National Research Foundation (R279-000-444-281 and R279-000-483-281), the National University of Singapore (R279-000-482-133) for financial support. This work was also supported by City University of Hong Kong (CityU Internal Funds for External Grant Schemes (9678157) and CityU Applied Research Grant: Project no. 9667160).

Keywords: antibacterial activity • aggregation-induced emission • membrane anchor • photodynamic antimicrobial therapy •

[1] a) K. A. Brogden, *Nat. Rev. Microbiol*. **2005**, 3, 238-250; b) J. M. Blair, M. A. Webber, A. J. Baylay, D. O. Ogbolu, L. J. Piddock, *Nat. Rev. Microbiol*. **2015**, 13, 42-51.

[2] a) X. Li, S. Lee, J. Yoon, *Chem. Soc. Rev*. **2018**, 47, 1174-1188; b) F. Cieplik, D. Deng, W. Crielaard, W. Buchalla, E. Hellwig, A. Al-Ahmad, T. Maisch, *Crit. Rev. Microbiol*. **2018**, 44, 571-589; c) X. Li, H. Bai, Y. Yang, J. Yoon, S. Wang, X. Zhang, *Adv. Mater*. **2019**, 31, e1805092; d) L. Dijkshoorn, A. Nemec, H. Seifert. *Nat. Rev. Microbiol.* **2007**, 5, 939-951; e) Y. Liu, R. Qin, S. Zaat, E. Breukink, M. Heger. *J. Clini. and Trans. Res.* **2015**.1(3); 140-167.

[3] K. Lagerstedt, *World Economic Forum*, **2019**.

[4] a) D. Mao, F. Hu, Kenry, S. Ji, W. Wu, D. Ding, D. Kong, B. Liu, *Adv. Mater*. **2018**, 30, e1706831; b) W. Wu, D. Mao, F. Hu, S. Xu, C. Chen, C. J. Zhang, X. Cheng, Y. Yuan, D. Ding, D. Kong, B. Liu, *Adv. Mater*. **2017**, 29; c) W. Wu, D. Mao, X. Cai, Y. Duan, F. Hu, D. Kong, B. Liu, *Chem. Mater*. **2018**, 30, 3867-3873; d) W. Wu, D. Mao, S. Xu, S. Ji, F. Hu, D. Ding, D. Kong, B. Liu, *Mater. Horiz*. **2017**, 4, 1110-1114; e) S. Wang, W. Wu, P. Manghnani, S. Xu, Y. Wang, C. C. Goh, L. G. Ng, B. Liu, *ACS nano* **2019**, 13, 3095-3105; f) S. Xu, W. Wu, X. Cai, C. J. Zhang, Y. Yuan, J. Liang, G. Feng, P. Manghnani, B. Liu, *Chem Commun.* **2017**, 53, 8727-8730; g) F. Hu, S. Xu, B. Liu, *Adv. Mater*. **2018**, 30, 1801350; h) F. Hu, Y. Huang, G. Zhang, R. Zhao, H. Yang, D. Zhang, *Anal. Chem*. **2014**, 86, 7987-7995; i) G. Feng, Y. Yuan, H. Fang, R. Zhang, B. Xing, G. Zhang, D. Zhang, B. Liu, *Chem. Commun*. **2015**, 51, 12490-12493; j) F. Hu, D. Mao, X. Cai, W. Wu, D. Kong, B. Liu, *Angew. Chem.* **2018**, 130, 10339-10343; k) M. Gao, Q. Hu, G. Feng, N. Tomczak, R. Liu, B. Xing, B. Z. Tang, B. Liu, *Adv. Healthc. Mater*. **2015**, 4, 659-663; i) M. R. Detty, S. L. Gibson, S. J. Wagner, *J. Med. Chem*. **2004**, 47, 3897-3915; m) H. Zhu, J. Li, X. Qi, P. Chen, K. Pu, *Nano Lett*. **2018**, 18, 586-594; n) Walsh, C. D.; Zheng, G. *Angew. Chem. Int. Ed*. **2019**, 58, 2558-2569; o) H. Yuan, B. Wang, F. Lv, L. Liu, S. Wang, Adv Mater **2014**, 26, 6978-6982.

[5] a) A. Garcia-Sampedro, A. Tabero, I. Mahamed, P. Acedo, *J. Porphyr. Phthalocya.* **2019**, 23, 11-27; b) M. Wainwright, K. B. Crossley, *J. Chemother*. **2002**, 14, 431-443.

[6] a) C. J. Zhang, Q. L. Hu, G. X. Feng, R. Y. Zhang, Y. Y. Yuan, X. M. Lu and B. Liu, *Chem. Sci.* **2015**, 6, 4580-4586; b) Q. Hu, M. Gao, G. Feng, B. Liu, *Angew. Chem. Int. Ed*. **2014**, 53, 14225-14229.

[7] a) Z. Zhou, J. Song, L. Nie, X. Chen, *Chem. Soc. Rev*. **2016**, 45, 6597-6626; b) X. Zhen, J. Zhang, J. Huang, C. Xie, Q. Miao, K. Pu, *Angew. Chem. Int. Ed.* **2018**, 57, 7804-7808.

[8] a) E. Zhao, Y. Chen, H. Wang, S. Chen, J. W. Lam, C. W. Leung, Y. Hong, B. Z. Tang, *ACS Appl. Mater. Interfaces* **2015**, 7, 7180-7188; b) W. Zhang, Y. Huang, Y. Chen, E. Zhao, Y. Hong, S. Chen, J. W. Y. Lam, J. Hou, B. Z. Tang, *ACS Appl. Mater. Interfaces* **2019**, 11, 10567-10577.

[9] a) B. Wang, M. Wang, A. Mikhailovsky, S. Wang, G. C. Bazan, *Angew. Chem. Int. Ed*. **2017**, 56, 5031-5034; b) A. W. Thomas, Z. B. Henson, J. Du, C. A. Vandenberg, G. C. Bazan, *J. Am. Chem. Soc*. **2014**, 136, 3736-3739.

[10] H. Bai, H. Yuan, C. Nie, B. Wang, F. Lv, L. Liu, S. Wang, *Angew. Chem. Int. Ed*. **2015**, 54, 13208-13213.

[11] a) I. Jelesarov, H. R. Bosshard, *J. Mol. Recognit*. **1999**, 12, 3-18; b) K. Liu, Y. Liu, Y. Yao, H. Yuan, S. Wang, Z. Wang, X. Zhang, *Angew. Chem. Int. Ed*. **2013**, 125, 8443-8447.

[12] a) H. Yan, C. Catania, G. C. Bazan, *Adv. Mater*. **2015**, 27, 2958-2973; b) H. Chen, M. Li, Z. Liu, R. Hu, S. Li, Y. Guo, F. Lv, L. Liu, Y. Wang, Y. Yi, *Sci. China Chem*. **2018**, 61, 113-117; c) H. Yuan, Z. Liu, L. Liu, F. Lv, Y. Wang, S. Wang, *Adv. Mater.* **2014**, 26, 4333-4338.

[13] a) C. Zhu, Q. Yang, L. Liu, F. Lv, S. Li, G. Yang, S. Wang, *Adv. Mater*. **2011**, 23, 4805-4810; b) C. Xing, Q. Xu, H. Tang, L. Liu, S. Wang, *J. Am. Chem. Soc.* **2009**, 131, 13117-13124.

[14] a) M. S. Butler, M. A. Cooper, *J Antibiot* (Tokyo) **2011**, 64, 413-425; b) D. J. Farrell, M. Robbins, W. Rhys-Williams, W. G. Love, *Int. J. Antimicrob. Agents,* **2010**, 35, 531-536.

[15] a) T. Maisch, C. Bosl, R. M. Szeimies, N. Lehn, C. Abels, *Antimicrob. Agents Chemother.* **2005**, 49, 1542-1552; b) T. Maisch, A. Eichner, A. Spath, A. Gollmer, B. Konig, J. Regensburger, W. Baumler, *PLoS One* **2014**, 9, e111792.

10.1002/anie.201907343

WILEY-VCH

Entry for the Table of Contents

COMMUNICATION

A membrane anchor (**TBD-anchor**) photosensitizer with aggregation-induced emission provides highly efficient $^1O_2$ generation specifically on bacteria membrane. Over 99.8% killing efficiency was obtained for *MRSA* when they were exposed to 0.8 μM of **TBD-anchor**. **TBD-anchor** thus shows great promise as an effective antimicrobial agent to combat the menace of multidrug-resistant bacteria.

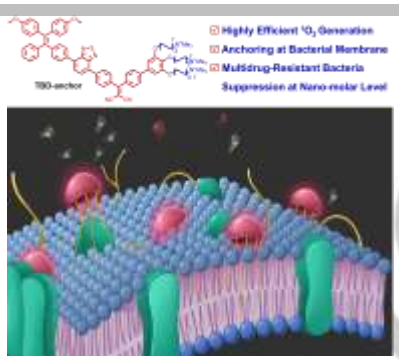

Huan Chen, Shengliang Li, Min Wu, Kenry, Zhongming Huang, Prof. Chun-Sing Lee*, and Prof. Bin Liu**

Page No. – Page No.

Membrane-Anchoring Photosensitizer with Aggregation-Induced Emission Characteristics for Combating Multidrug-Resistant Bacteria